ARTICLES
PUBLISHED ONLINE: 20 NOVEMBER 2011 | DOI: 10.1038/NCHEM.1199
nature chemistry

Broken symmetry and the variation of critical properties in the phase behaviour of supramolecular rhombus tilings

Andrew Stannard[1]*, James C. Russell[1], Matthew O. Blunt[1], Christos Salesiotis[2], María del Carmen Giménez-López[2], Nassiba Taleb[2], Martin Schröder[2], Neil R. Champness[2], Juan P. Garrahan[1] and Peter H. Beton[1]*

The tiling of surfaces has long attracted the attention of scientists, not only because it is intriguing intrinsically, but also as a way to control the properties of surfaces. However, although random tiling networks are studied increasingly, their degree of randomness (or partial order) has remained notoriously difficult to control, in common with other supramolecular systems. Here we show that the random organization of a two-dimensional supramolecular array of isophthalate tetracarboxylic acids varies with subtle chemical changes in the system. We quantify this variation using an order parameter and reveal a phase behaviour that is consistent with long-standing theoretical studies on random tiling. The balance between order and randomness is driven by small differences in intermolecular interaction energies, which can be related by numerical simulations to the experimentally measured order parameter. Significant variations occur with very small energy differences, which highlights the delicate balance between entropic and energetic effects in complex self-assembly processes.

Two-dimensional (2D) molecular networks provide an attractive and highly flexible route to the formation of surfaces with specific structural arrangements and functionalities[1,2]. Within the broad range of structures explored, random molecular networks have gained considerable attention recently as exemplars of 2D, non-periodic glassy systems[3–6]. Although these systems are of great interest and represent examples of complex self-assembled architectures a quantitative measure of the degree of randomness present in a molecular array is not generally available. In this paper we report a set of supramolecular arrays in which the randomness varies as a result of small changes in the chemical environment or molecular geometry. We define an order parameter that quantifies these variations and enables a systematic comparison between supramolecular arrays prepared using similar methodologies. Furthermore, we show that the observed variations may be rationalized within a complex phase diagram, which can be related to the adsorption of dimers on a periodic lattice[7,8]. This classic problem in statistical mechanics has been studied for several decades and is a well-known example of a physical system that can be mapped onto a non-periodic tiling of the plane[9–16]. In particular, using numerical simulations we related the order parameter to an orientational dependence of the intermolecular interactions that stabilize the network.

We focused on molecular rhombus tilings that formed at the liquid–solid interface after deposition of the solvated molecules of interest on highly oriented pyrolytic graphite (HOPG) substrates. In recent work we showed[3] that such arrays support the formation of a random tiling and represent an experimental realization of the dimer-adsorption problem. The molecular networks formed on graphite were imaged using scanning tunnelling microscopy (STM) and the observed structures mapped directly onto rhombus tilings. The images, tilings and molecular structures are shown in Fig. 1. In-plane stabilization of the molecular networks arises from hydrogen bonds formed between carboxylic acid groups[6,17,18]. For the tetracarboxylic acids considered here this results in two orientations of intermolecular bonding with the molecular backbone axes, either parallel or non-parallel at 60°, as shown in Fig. 1a. To form a random tiling a close match between the two dimensions, marked d_1 and d_2 in Fig. 1a, is required. Examples of suitable molecules are *p*-terphenyl-3,5,3″,5″-tetracarboxylic acid (TPTC) (Fig. 1j), with $d_1 = 8.7$ Å, which we studied previously[3], and 1,4-diphenyl-1,3-butadiyne-3,3″,5,5″-tetracarboxylic acid (DPBDTC) (Fig. 1i), with $d_1 = 9.5$ Å, synthesized specifically for this study; $d_2 = 9.6$ Å for both molecules. Several closely related molecules studied previously[6,17–19] do not display an extended random tiling, although frustrated crystallization has been observed[6]. To tile the plane perfectly a rhombus must have internal angles of 60° and 120° (referred to as a lozenge[11]), for which $d_1 = d_2$.

A random tiling is considered ideal when the energies of the non-parallel and parallel alignments, given by ε_N and ε_P, respectively, are degenerate ($\varepsilon_N = \varepsilon_P$) (refs 13–16). In this case, the tiling configuration is determined solely by maximizing the configurational entropy. Such tilings possess no translational order and display correlations in tile orientation that have a logarithmic dependence on spatial separation, a signature of a 'Coulomb' phase[9]. However, if there is an energetic asymmetry, $\Delta = \varepsilon_N - \varepsilon_P \neq 0$, the degeneracy between the exponentially large number of tilings is broken. In this case, an additional internal energy contribution to the free energy competes with the entropic term (rhombus tiles with asymmetric interactions are described as interacting in many theoretical models[13–16]). For small Δ, random-tiling phases (with properties that vary continuously with Δ) are expected, but large Δ values are predicted to lead to transitions to ordered phases[13–16]. The parameter Δ can be considered as analogous to the coupling constant J that

[1]School of Physics and Astronomy, University of Nottingham, University Park, Nottingham NG7 2RD, UK, [2]School of Chemistry, University of Nottingham, University Park, Nottingham NG7 2RD, UK. *e-mail: andrew.stannard@nottingham.ac.uk; peter.beton@nottingham.ac.uk

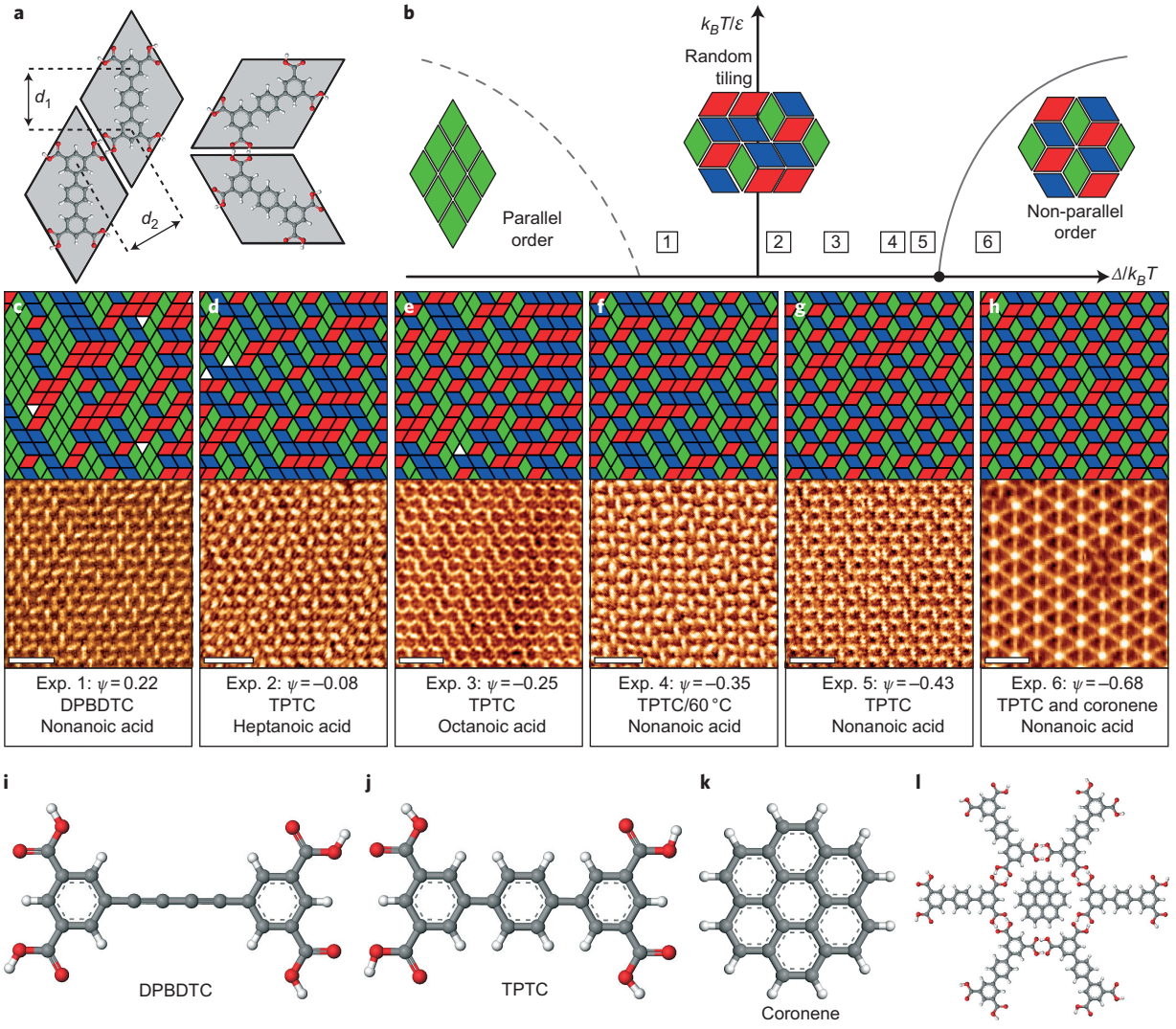

Figure 1 | Tetracarboxylic acid supramolecular assemblies and rhombus tilings. a, Parallel and non-parallel intermolecular bonding orientations, with backbone (d_1) and bond (d_2) lengths indicated, overlaid onto the corresponding representations of the rhombus tiles. **b**, Schematic phase diagram of the interacting rhombus tiling model. Three phases are expected depending on the interaction energy Δ: a random-tiling phase, an ordered phase dominated by non-parallel bonding at large positive Δ and a second ordered phase dominated by parallel bonding at large negative Δ. **c**–**h**, STM images (sections of larger area scans) of tetracarboxylic acid supramolecular networks at alkanoic acid–HOPG interfaces and the corresponding rhombus tilings, in a sequence of decreasing Ψ. Experiments are labelled 1–6 and were performed at room temperature (apart from Experiment 4, which was at 60 °C) using different combinations of TPTC, DPBDTC, coronene and solvents, as specified in the text boxes. STM image contrast originates from molecular backbones and, in **h**, coronene (see Methods for imaging parameters; all scale bars = 50 Å). **i**–**k**, Molecular ball-and-stick diagrams of DPBDTC (**i**), TPTC (**j**) and coronene (**k**). **l**, Diagram of coronene adsorbed at the vertex of six TPTC molecules.

appears in Ising models of magnetism and leads to ordered phases with broken symmetry for $|J| \gtrsim k_BT$, where k_B is the Boltzmann constant and T the temperature; these phases may be either ferromagnetic or antiferromagnetic depending on the sign of J, although entropic terms in the free energy dominate for $|J| \ll k_BT$, in which case a paramagnetic phase occurs. Our experiments and simulations show that this rich phase behaviour may be investigated by preparing molecular arrays with differing values of Δ.

Results and discussion

Figure 1c–h shows images of molecular networks prepared under several different conditions (see Methods), referred to as Experiments 1–6, respectively, and the corresponding representations of rhombus tiling, in which each molecule is represented by a rhombus coloured according to its orientation. To characterize our experimental tilings we defined an order parameter, $\Psi = (n_0p - p_0n)/(n_0p + p_0n)$, where n and p represent the fraction of rhombus tile junctions in non-parallel and parallel orientations, respectively, and $n_0 = 0.608$ and $p_0 = 0.392$ are the equivalent values for a defect-free, ideal, random tiling and were estimated numerically (see Methods). As such, Ψ equals 1 in a fully parallel phase, -1 in a fully non-parallel phase and 0 for an ideal random tiling. Ψ was calculated for each of Experiments 1–6; the images in Fig. 1c–h are placed in order of decreasing Ψ, from $\Psi = 0.22$ to $\Psi = -0.68$.

Figure 1b is a schematic of the expected equilibrium phase diagram[13–16]. The two relevant thermodynamic parameters are temperature, T (in units of ε, the characteristic hydrogen bond energy) and energetic bias, Δ. Ideal random tilings are observed for $\Delta = 0$. For $\Delta > 0$, non-parallel bonding is favoured, which results in increasingly negative values of Ψ. For sufficiently large Δ the system orders into a crystalline phase dominated by non-parallel bonds. This transition occurs at $\Delta/k_BT = 0.454(3)$, a value calculated in the limit of zero temperature and the transition is of the Kosterlitz–Thouless kind[16]. For non-zero temperatures of

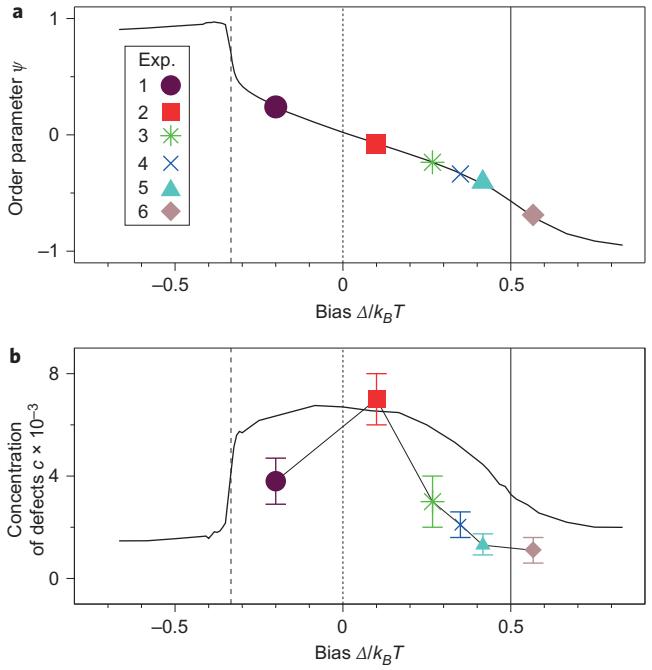

Figure 2 | Comparison of experiments with simulations of the rhombus-tiling model. a, Order parameter Ψ as a function of scaled bias Δ/k_BT. The full curve is the result of numerical simulations of the rhombus-tiling model (see Methods) for $\varepsilon_N/k_BT = 5/3$ (at this value the concentration of defects c is comparable to that observed experimentally). The vertical lines indicate the first-order transition to the parallel phase, $\Delta/k_BT = -0.34(3)$ and the approximate location of the continuous transition to the non-parallel ordered phase, $\Delta/k_BT = 0.49(2)$, slightly larger than that calculated[16] for $T = 0$ (see Methods; for non-zero temperatures, the transition is second order and occurs at slightly larger values of Δ/k_BT). The experimental points are placed on the curve according to the measured values of Ψ. **b**, Concentration of defects as a function of bias. The full curve is the numerical result. The abscissa values for experimentally measured defect concentrations are determined from (**a**). The simplicity of the model meant that we did not try to overfit the data, but the suppression of defect formation in the ordered phases, which shows the predicted non-monotonic dependence on bias, is reproduced in our experiments.

relevance to our experiments and simulations, the transition is second order and occurs at slightly larger values of Δ/k_BT. For $\Delta < 0$ parallel bonding is favoured, which results in increasingly positive values of Ψ. The random-tiling phase extends until $\Delta/k_BT \approx -0.3$, where the system undergoes a first-order transition[15] to a crystalline phase dominated by parallel bonds. We reiterate the analogy with magnetic systems in which transitions from disordered to ordered phases occur when the absolute value of the coupling constant is increased beyond some critical value.

It is clear from Fig. 1 that different experimental conditions give rise to tilings with varying degrees of order. In Experiment 1 we investigated DPBDTC in nonanoic acid (Fig. 1c). For this arrangement there were more parallel bonds than expected for an ideal random tiling and $\Psi = 0.22$. A solution of TPTC in heptanoic acid (Experiment 2, Fig. 1d) resulted in a molecular tiling with $\Psi = -0.08$. This is the molecular tiling closest to ideal (that is, $\Psi = 0$) of all the systems we studied. For TPTC, a change of solvent[20,21] from heptanoic acid to solvent molecules with similar chemistry but slightly larger size, namely octanoic acid (Experiment 3, Fig. 1e, $\Psi = -0.25$) or nonanoic acid (Experiment 5, Fig. 1g, $\Psi = -0.43$), led to a progressive increase in the fraction of non-parallel bonds. Experiment 4 was performed with TPTC and nonanoic acid at an elevated temperature of 60 °C (Fig. 1f, $\Psi = -0.35$). Comparison of this molecular tiling with the equivalent tiling prepared at 19 °C (room temperature) shows that the increase in temperature led, as expected, to a value of Ψ closer to zero. Finally, the most negative order parameter, $\Psi = -0.68$, was observed when coronene (Fig. 1k) was added to a solution of TPTC and nonanoic acid (Experiment 6, Fig. 1h). Coronene becomes incorporated in the molecular network at a site that enhances the stabilization of the non-parallel arrangement (Fig. 1l), a capture process consistent with previous studies of coronene–carboxylic acid and other systems[19,22–24].

These results show that small modifications in experimental parameters lead to the exploration of the phase space of the rhombus-tiling model. To determine the placement of the experimental structures on the phase diagram in Fig. 1b, we undertook extensive numerical simulations of rhombus tilings. The details of the numerical scheme are provided in the Methods section and represent a generalization of previous work[25,26] to the case $\Delta \neq 0$. Figure 2a shows the numerically computed order parameter Ψ as a function of scaled bias Δ/k_BT. Vertical lines indicate where the transitions from random to ordered phases occur. The six experiments are marked on the numerical curve according to their measured Ψ values. Experiments 2–5 span the random-tiling region with negative Ψ, Experiment 6 lies beyond the phase boundary in the non-parallel phase and Experiment 1 is close to the phase boundary with the ordered parallel phase.

The numerical results in Fig. 2a provide a relationship between the order parameter Ψ and Δ/k_BT, which allows an estimation of the latter for each of our experiments. Furthermore, using the known temperature at which the experiments were performed we can estimate values of Δ (Table 1). A comparison of Experiments 4 and 5 is of particular interest: both were performed using TPTC in nonanoic acid, but with molecular networks prepared at different temperatures. Accordingly, we anticipated the same value of Δ and found excellent agreement with the values inferred from simulations. This result provides strong support for our analysis and confirmation that the molecular arrays can be understood in terms of equilibrium structures. From our experiments it is clear that measurable variations in the tiling statistics may be identified even for variations of Δ lower than ~5 meV, much less than the thermal energy at room temperature.

A second experimental measure, which can also be compared with numerical results, is the concentration of defects. These 'half-rhombus' vacancies are topological defects and are present in several of the images shown in Fig. 1. For an ideal tiling their

Table 1 | Estimate of the energy Δ.

Parameter	Experiment number					
	1	2	3	4	5	6
Ψ	0.220(7)	−0.08(1)	−0.25(2)	−0.351(6)	−0.427(5)	−0.675(8)
Δ/k_BT	−0.182(5)	0.10(1)	0.280(9)	0.364(5)	0.421(3)	0.553(4)
Δ (meV)	−4.6(1)	2.7(3)	7.0(2)	10.5(1)	10.60(8)	13.9(1)

The energy was estimated from a comparison of the experimental and numerical results. The parameter Δ is inferred from Fig. 2a for each experimental system. The values are all less than the thermal energy at room temperature. Δ for Experiments 4 and 5, which correspond to the same system (TPTC in nonanoic acid) at different temperatures, is the same within experimental error, as expected.

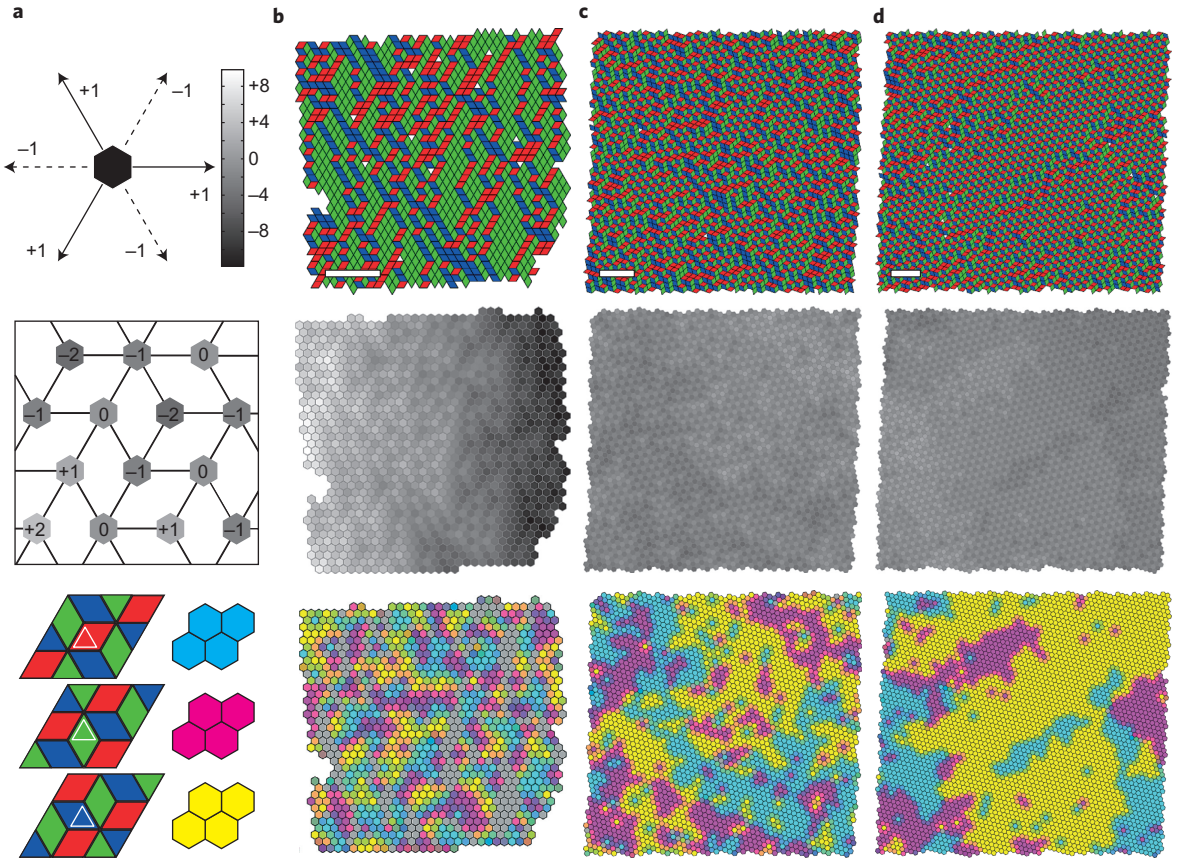

Figure 3 | Spatial variation of ordered phases. a, Vertices of rhombus tilings are assigned an effective height with changes of ± 1 for displacements along edges with different orientations (top). An illustrative example is shown in (middle). Heights are represented by greyscale (top). **b**–**d**, Results for Experiments 1 (**b**), 4 (**c**) and 6 (**d**), in each case as a tiling (top), height field representation (middle) and phase-domain representation (bottom). In (**b**) there is a bright to dark contrast variation close to the ordered parallel phase. No overall contrast variation is observed for Experiments 4 and 6, although the height fluctuations are greater for Experiment 4 (as expected for the random phase). In the phase-domain representation we map the spatial variation of the three possible sublattices of the non-parallel ordered phase, which are distinguished by the covering of any specific location, for example the highlighted triangle in (**a**, bottom), by a tile oriented in one of three directions, as indicated by cyan, magenta and yellow colourization. The domains are smallest for Experiment 1 (**b**, bottom), larger in Experiment 4 (**c**, bottom) and for Experiment 6 (**d**, bottom), in the non-parallel ordered phase, the domain size is comparable with the size of the system. Scale bar = 10 nm for all images.

concentration, c, has been shown to be temperature dependent[25] (we chose an effective temperature in our simulations to match, approximately, the maximum defect density observed in experiments) and Fig. 2b shows that c is also controlled by Δ. We highlight the non-monotonic dependence on bias that results from the strong suppression of isolated triangular defects in the ordered phases. The experimentally determined defect data are plotted against the theoretical curve using the value of Δ/k_BT obtained from Fig. 2a. The simplicity of the model meant we did not try to overfit the experimental data, but the non-monotonic behaviour and suppression of defect formation in the ordered phases are reproduced in our data, which thus provides further support for the validity of our approach to determine the value of Δ for our experiments.

Further analysis of our images shows explicitly the difference between random and ordered phases. Figure 3 shows images of larger areas for Experiments 1, 4 and 6, in three different representations. In addition to the tiling representation we also used a height representation: commonly, rhombus tilings are analysed using a simple transformation in which an effective height[9] $h(x,y)$ is assigned to each vertex (x and y are the in-plane coordinates of the vertex). This was achieved using the simple procedure outlined in Fig. 3a (top and middle), in which a step along a rhombus edge results in a change in height of ± 1 depending on the orientation of the edge. By defining an arbitrary zero it is possible to assign heights as shown in Fig. 3a (top). For the special case of the parallel ordered phase we would expect $h(x,y)$ to increase (or decrease) monotonically across the surface because all rhombi are oriented in the same direction. In contrast, for the non-parallel ordered phase, $h(x,y)$ is expected, on average, to be constant with fluctuations limited to ± 1. For the random tiling the average value of $h(x,y)$ is expected to be constant, but the fluctuations around this constant value would be larger than those observed in the ordered non-parallel phase.

Using this approach we converted the experimentally determined large-area tilings shown in Fig. 3b–d for Experiments 1 (Fig. 3b, top), 4 (Fig. 3c, top) and 6 (Fig. 3d, top) into height maps, which are represented as greyscale images using the scaling shown in Fig. 3a (top). Experiment 1 shows a clear height-contrast gradient (Fig. 3b, middle), which varies from bright on the left to dark on the right. This indicates that this experiment is close to the phase boundary to the parallel phase. However, the height maps for Experiments 4 (Fig. 3c, middle) and 6 (Fig. 3d, middle) show no overall contrast variation. As discussed above, this behaviour is expected for both the random and non-parallel ordered phases, although these can be distinguished by the greater height fluctuations present for Experiment 4, consistent with a random-tiling phase.

The third representation illustrates the spatial variation of non-parallel order. In a perfectly non-parallel configuration the unit

cell (as in the schematic inset of Fig. 1b, for example) can be centred at any of the three sublattices of the triangular lattice. This is illustrated in Fig. 3a, bottom in which small regions of the non-parallel ordered phase cover a region of the surface in three non-equivalent arrangements. In particular, a given location, for example the highlighted triangle, can be covered by a rhombus pointing in one of three directions. This identification can be used to classify which of the three sublattices is present at a particular region of the surface, represented by the three colours cyan, magenta and yellow. Choosing a sublattice is the symmetry breaking associated with the transition to the non-parallel phase and, in general, we would expect to observe domains of non-parallel order that correspond to each of these three possible sublattices. Again, a magnetic analogue is useful; in a ferromagnetic system domains of spin-up and spin-down magnetization are formed, the sizes of which diverge as the system undergoes a transition from a paramagnetic to a ferromagnetic phase. For the case considered here, there are three equivalent non-parallel ordered states into which the system can crystallize, rather than the two states available for a simple magnetic system.

Maps of the three possible non-parallel phases are shown in bottom panels of Fig. 3b–d. In Experiment 1 these domains were relatively small because the parallel tile alignment predominates (Fig. 3b, bottom). The domains in the random-tiling phase were larger but finite (Experiment 4, Fig. 3c, bottom). In Experiment 6 one domain became dominant and was comparable with the size of the system (Fig. 3d, bottom), which indicates a transition to the non-parallel phase.

Our results show conclusively that the phase space of 2D rhombus tiles, which arises from asymmetric interactions, may be explored experimentally through the structural characterization of molecular arrays. The changes in energy that give rise to different ordering are small compared to the thermal energy, an essential requirement for systems in which entropy is significant. The dependence of the characteristic energetic bias, Δ, on solvent indicates that the effective energetic difference between parallel and non-parallel molecular pairs adsorbed on graphite cannot be described simply by the interactions between two tetracarboxylic acid molecules and must include other more complex contributions.

We highlight two possible influences of the solvent molecules on the effective interaction between adsorbed molecules. Firstly, the coadsorption of solvent molecules on the graphite surface is possible[27,28], and expected, because the network of tetracarboxylic acid molecules results in an array of nanopores that can accommodate guest molecules. As shown in a recent paper[29], these nanopores are hexagonal and may be classified into five inequivalent types formed from different combinations of parallel and non-parallel bonded molecular pairs. There is a significant variation in the capture of guest molecules in pores of different type[30], and we therefore also expect variations in the stabilization energies of the coadsorption of solvent molecules in different pore types. The energy of coadsorbed molecules makes a contribution to the overall stability[27] of a given pore, so this effect provides a mechanism that breaks the degeneracy of the different pore types. As different pores are formed by different combinations of parallel and non-parallel pairs, variations in guest-inclusion stability will result in small effective energetic differences between the parallel and non-parallel molecular orientations. A second consideration is that solvents provide an effective medium of varying dielectric constant, as pointed out by Kampschulte *et al.*[20], which would give rise to a solvent dependence of any energetic imbalance between neighbouring molecules mediated, for example, by van der Waals interactions or hydrogen bonding (see Cook *et al.*[30] for a discussion of solvent effects on intermolecular interactions in a solution environment). For a significant mismatch between d_1 and d_2 we expect the parallel ordered phase previously reported for an analogue molecule with $d_1 \gg d_2$ (ref. 19).

A complete microscopic description of energy differences on this scale is beyond the confidence levels normally associated with modern numerical approaches to molecular modelling (for example, density functional theory, molecular dynamics). Furthermore, the inclusion of solvent molecules makes a detailed microscopic description and prediction of energies particularly problematic. However, our experiments give clear limits on the tolerance of the random-tiling phase to symmetry breaking: a difference in binding energies of $\gtrsim 10$ meV will drive the structures into an ordered phase.

Our study demonstrates that prototypical self-assembled systems, such as supramolecular networks, can reveal a richness of exotic phases already studied widely by theorists and are analogous to those found in complex condensed-matter systems. In addition, our work highlights the role of entropy in the balance between order and disorder in molecular templates.

Methods

Chemicals. DPBDTC and TPTC were synthesized in-house, details of which are given in the accompanying Supplementary Information and in Blunt *et al.*[3], respectively. Other chemicals used were coronene (≥95.0%, Fluka), heptanoic acid (≥97%, Sigma), octanoic acid (≥98%, Aldrich) and nonanoic acid (≥95%, Fluka).

STM experiments. STM images were acquired with an Agilent Technologies 4500 PicoPlus STM using a PicoScan controller and STM tips formed from mechanically cut PtIr (80:20) wire. Saturated solutions of the adsorbate (DPBDTC or TPTC) were prepared by placing an excess of solid in the desired solvent (heptanoic, octanoic or nonanoic acid). For Experiment 6, the solution used combined equal volumes of a saturated solution of TPTC in nonanoic acid and coronene in nonanoic acid (1.5×10^{-4} mg ml^{-1}). All solutions were agitated ultrasonically to ensure complete dissolution. To form the supramolecular networks, a droplet (10 μl) of solution was deposited onto a mechanically cleaved HOPG substrate. Imaging at the alkanoic acid–HOPG interface commenced immediately after the approach of the STM tip. For Experiment 4, the substrate was heated to 60 °C prior to solution deposition and held at this temperature for the duration of the experiment. Figure 1 STM imaging parameters (V_{tip}/I) were: 1c, +1.1 V/10 pA; 1d, +1.2 V/15 pA; 1e, +1.2 V/5 pA; 1f, +1.25 V/12 pA; 1g, +1.0 V/13.5 pA; 1h, +1.0 V/30 pA.

Numerical simulations. The rhombus tilings were simulated using the same model as used by Garrahan *et al.*[25] supplemented by interactions that varied depending on whether neighbouring tiles were non-parallel (binding energy ε_N, held fixed) or parallel (binding energy ε_P, set equal to $\varepsilon_N - \Delta$). Simulations were performed with continuous-time Monte Carlo, which allows access to very long times at low temperatures (that is, a very low number of defects) on system sizes from $N = 18^2$ to $N = 99^2$ and averaged over 10^3 samples for each state point. The location of the continuous transition from the random tiled to the ordered non-parallel phase at $T \neq 0$ (the location at $T = 0$ is known exactly[16]) was determined from finite size-scaling analysis of susceptibilities and higher order cumulants of Ψ and of the 'columnar' order parameter (difference in density of non-parallel order in each sublattice), as in Alet *et al.*[13]; for the location of the first-order transition to the ordered parallel phase from the jump in Ψ and the 'tilt' order parameter (difference in density of each kind of tile), see Castelnovo *et al.*[15].

Received 4 July 2011; accepted 12 October 2011; published online 20 November 2011

References

1. Elemans, J. A. A. W., Lei, S. & De Feyter, S. Molecular and supramolecular networks on surfaces: from two-dimensional crystal engineering to reactivity. *Angew. Chem. Int. Ed.* **48,** 7298–7332 (2009).
2. Bartels, L. Tailoring molecular layers at metal surfaces. *Nature Chem.* **2,** 87–95 (2010).
3. Blunt, M. O. *et al.* Random tiling and topological defects in a two-dimensional molecular network. *Science* **322,** 1077–1081 (2008).
4. Otero, R. *et al.* Elementary structural motifs in a random network of cytosine adsorbed on a gold(111) surface. *Science* **319,** 312–315 (2008).
5. Marschall, M. *et al.* Random two-dimensional string networks based on divergent coordination assembly. *Nature Chem.* **2,** 131–137 (2010).
6. Zhou, H. *et al.* Frustrated 2D molecular crystallization. *J. Am. Chem. Soc.* **129,** 13774–13775 (2007).
7. Fisher, M. E. Statistical mechanics of dimers on a plane lattice. *Phys. Rev.* **124,** 1664–1672 (1961).
8. Kasteleyn, P. W. Dimer statistics and phase transitions. *J. Math. Phys.* **4,** 287–297 (1963).
9. Henley, C. L. in *Quasicrystals, the State of the Art* (eds Di Vincenzo, D. P. & Steinhardt, P. J.) Ch. 15 (World Scientific, 1999).

10. Destainville, N. Flip dynamics in octagonal rhombus tiling sets. *Phys. Rev. Lett.* **88,** 030601 (2002).
11. Wilson, D. B. Mixing times of lozenge tiling and card shuffling Markov chains. *Ann. Appl. Probab.* **14,** 274–325 (2004).
12. Lu, P. J. & Steinhardt, P. J. Decagonal and quasi-crystalline tilings in medieval Islamic architecture. *Science* **315,** 1106–1110 (2007).
13. Alet, F., Ikhlef, Y., Jacobsen, J. L., Misguich, G. & Pasquier, V. Classical dimers with aligning interactions on the square lattice. *Phys. Rev. E* **74,** 041124 (2006).
14. Papanikolaou, S., Luijten, E. & Fradkin, E. Quantum criticality, lines of fixed points, and phase separation in doped two-dimensional quantum dimer models. *Phys. Rev. B* **76,** 134514 (2007).
15. Castelnovo, C., Chamon, C., Mudry, C. & Pujol, P. Zero-temperature Kosterlitz–Thouless transition in a two-dimensional quantum system. *Ann. Phys.* **322,** 903–934 (2007).
16. Jacobsen, J. L. & Alet, F. Semiflexible fully packed loop model and interacting rhombus tilings. *Phys. Rev. Lett.* **102,** 145702 (2009).
17. Lackinger, M. & Heckl, W. M. Carboxylic acids: versatile building blocks and mediators for two-dimensional supramolecular self-assembly. *Langmuir* **25,** 11307–11321 (2009).
18. Zhao, J. F. *et al.* Molecule length directed self-assembly behaviour of tetratopic oligomeric phenylene–ethynylenes end-capped with carboxylic groups by scanning tunneling microscopy. *J. Phys. Chem. C* **114,** 9931–9937 (2010).
19. Blunt, M. *et al.* Directing two-dimensional molecular crystallization using guest templates. *Chem. Commun.* 2304–2306 (2008).
20. Kampschulte, L. *et al.* Solvent induced polymorphism in supramolecular 1,3,5-benzenetribenzoic acid monolayers. *J. Phys. Chem. C* **110,** 10829–10836 (2006).
21. Tahara, K. *et al.* Two-dimensional porous molecular networks of dehydrobenzo[12]annulene derivatives via alkyl chain interdigitation. *J. Am. Chem. Soc.* **128,** 16613–16625 (2006).
22. Furukawa, S. *et al.* Structural transformation of a two-dimensional molecular network in response to selective guest inclusion. *Angew. Chem. Int. Ed.* **46,** 2831–2834 (2007).
23. Griessl, S. J. H. *et al.* Incorporation and manipulation of coronene in an organic template structure. *Langmuir* **20,** 9403–9407 (2004).
24. Wu, D., Deng, K., He, M., Zeng, Q. & Wang, C. Coadsorption-induced reconstruction of supramolecular assembly characteristics. *ChemPhysChem* **8,** 1519–1523 (2007).
25. Garrahan, J. P., Stannard, A., Blunt, M. O. & Beton, P. H. Molecular random tilings as glasses. *Proc. Natl Acad. Sci. USA* **106,** 15209–15213 (2009).
26. Stannard, A., Blunt, M. O., Beton, P. B. & Garrahan, J. P. Entropically stabilized growth of a two-dimensional random tiling. *Phys. Rev. E* **82,** 041109 (2010).
27. Gutzler, R. *et al.* Reversible phase transitions in self-assembled monolayers at the liquid–solid interface: temperature-controlled opening and closing of nanopores. *J. Am. Chem. Soc.* **132,** 5084–5090 (2010).
28. Yang, Y. and Wang, C. *Curr. Opin. Colloid Interface Sci.* **14,** 135–147 (2009).
29. Blunt, M. O. *et al.* Guest-induced growth of a surface-based supramolecular bilayer. *Nature Chem.* **3,** 74–78 (2011).
30. Cook, J. L., Hunter, C. A., Low, C. M. R., Perez-Velasco, A. & Vinter, J. G. Solvent effects on hydrogen bonding. *Angew. Chem. Int. Ed.* **46,** 3706–3709 (2007).

Acknowledgements

We thank the UK Engineering and Physical Sciences Research Council (EPSRC) for financial support under grant EP/D048761/01. J.P.G. was supported by EPSRC Grant No. GR/S54074/01. A.S. was supported by the Leverhulme Trust (ECF/2010/0380) and the EPSRC (EP/P502632/1). M.S. acknowledges receipt of a Royal Society Wolfson Merit Award and an European Research Council Advanced Grant. N.R.C. acknowledges receipt of a Royal Society Leverhulme Trust Senior Research Fellowship.

Author contributions

A.S., J.C.R., M.O.B., J.P.G., N.R.C. and P.H.B. designed and conceived the experiment, A.S., J.C.R. and M.O.B. performed the experiments, A.S. and J.P.G. performed the numerical simulations, C.S., M.C.G-L., N.T., M.S. and N.R.C. prepared the materials, A.S., J.P.G., M.O.B., J.C.R. and P.H.B. analysed the data, A.S., J.P.G. and P.H.B. co-wrote the paper and all authors provided revisions and comments on the manuscript.

Additional information

The authors declare no competing financial interests. Supplementary information accompanies this paper at www.nature.com/naturechemistry. Reprints and permission information is available online at http://www.nature.com/reprints. Correspondence and requests for materials should be addressed to A.S. and P.H.B.